

## EIGENMODE DECOUPLING FOR MIMO LOOP-ANTENNA BASED ON 180° COUPLER

S.-L. Zuo<sup>\*</sup>, Y.-Z. Yin, Z.-Y. Zhang, W.-J. Wu, and J.-J. Xie

Science and Technology on Antenna and Microwave Laboratory, Xidian University, Xi'an, Shaanxi, China

**Abstract**—A low-cost, high isolation, printed loop-antenna system for multiple-input multiple-output (MIMO) applications in the 2.4 GHz WLAN band is presented. By feeding the orthogonal eigenmodes of the array, port decoupling ( $S_{21} < -20$  dB) with tightly coupled elements (only  $0.07\lambda$  separation) is obtained. The orthogonal eigenmodes are realized based on 180° coupler. Then decoupled external ports of the feed network may be matched independently by using conventional matching circuits. With this low-cost and high isolation characteristic, it is very suitable for being embedded inside a wireless access point (AP).

### 1. INTRODUCTION

For well suiting for present-day APs of “11n” or “pre-n” compatible on the open market, the multiple-input multiple-output (MIMO) technology adopting multiple transmit/receive antennas to get higher throughput has become enormously popular [1]. The antenna design is important when multiple antennas are integrated into APs with limited device size. Noted that effects of mutual coupling become more severe when the inter-element spacing is reduced beyond half a wavelength. Achieving high isolation between closely-packed antenna elements is difficult to achieve and has been well studied [2–6]. In [2, 3], Diallo and Luxey improve the isolation by introducing a suspended line between the two planar inverted-F antennas (PIFAs). A quarter-wavelength slot was used in [4] to reduce mutual coupling at 5.0 GHz. Compared to a reference, the achieved reduction in mutual coupling was about 7 dB. In [5], reduction of mutual coupling was studied by using a quarter-wavelength slot between two compactly spaced monopole antennas.

---

*Received 11 July 2011, Accepted 9 August 2011, Scheduled 16 August 2011*

\* Corresponding author: Shaoli Zuo (zuoshaoli@163.com).

By using a 13.5 mm slot between the antennas, mutual coupling was reduced by approximately only 6 dB compared to a reference at a centre frequency of 3.5 GHz. In [6], Chiu et al. proposed slit pattern etched onto ground plane to reduce mutual coupling between closely-packed antenna elements and more than 20 dB can be achieved between two parallel individual planar inverted-F antennas (PIFAs). However, the using of the several pairs of slots makes the structure complicated. Decoupling networks have been implemented by connecting simple reactive elements between the input ports and antenna ports, but this is only applicable in special cases where the off-diagonal elements of the admittance matrix are all purely imaginary [7–9].

In this paper, a low-cost, high isolation, printed loop-antenna system for multiple-input multiple-output (MIMO) applications in the AP 2.4 GHz WLAN band is presented. It involves a modal feed network which makes use of the orthogonality of the eigenmodes of the array to achieve decoupling. By feeding the orthogonal eigenmodes of the array, port decoupling ( $S_{21} < -20$  dB) with tightly coupled elements (only  $0.07\lambda$  separation) is obtained. The orthogonal eigenmodes are realized based on  $180^\circ$  coupler. Then decoupled external ports of the feed network may be matched independently by using conventional matching circuits. Design considerations of the proposed antennas are described in the article. Results of the constructed prototype are presented and discussed.

## 2. LOOP-ANTENNA STRUCTURE

Figure 1(a) shows the configuration of the two loop-antenna system formed on FR4 substrate of thickness 1 mm and backed by a system ground plane of a wireless AP for WLAN2.4 band operation, which an

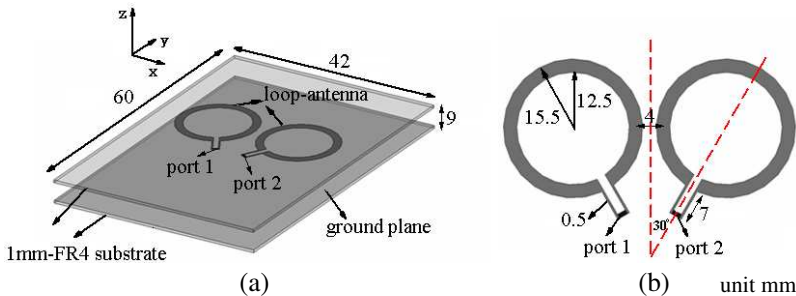


**Figure 1.** Configuration of the loop-antenna system (a) 3D view (b) Detailed dimensions of the loop-antenna.

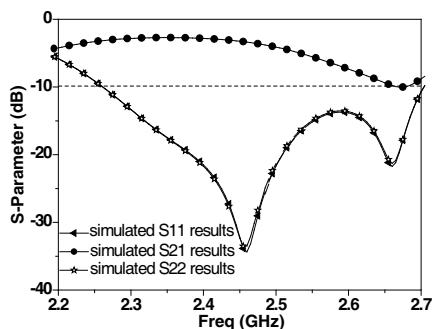


**Figure 2.** Simulated  $S$  parameters for the loop-antenna system.

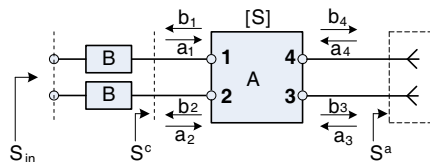


**Figure 3.** Feed network connected to the antenna array.

air separation between the two substrates. The ground plane can be utilized as an efficient reflector for the antennas, aiming more radiation in the direction to achieve directional radiation. Detailed dimensions of the two antennas are presented in Figure 1(b). The proposed antenna comprises a circular loop which operate at one-wavelength resonant mode. The central operating frequency is determined and controlled by the diameter of the loop. The width of the loop affects the antenna bandwidth, and in this study it is of uniform width of 3 mm. A thin pair of parallel strips for feeding have the effects on the input matching at 2.4 GHz with length 7 mm, width 0.5 mm. The distance between the two antennas is only 4 mm, which is about 0.07 wavelength at resonant frequency. Furthermore, the loop-antenna is rotated by a  $30^\circ$  degree rotation with respect to the center of the antenna substrate.

The simulated  $S$ -parameter against frequency is shown in Figure 2. From the figure, it can be observed that  $S_{11}$  are all less than  $-10$  dB (2380–2500 MHz). Due to the symmetry of the two antennas, the results of the  $S_{22}$  are as same as that of  $S_{11}$ . Over the 2.4 GHz band shown in the figure, it can be seen that the mutual coupling ( $S_{21}$ ) is strong, which is about  $-3$  dB due to the close separation between the two antennas.

### 3. STUDY WITH DECOUPLING NETWORK

Consider a 4-port passive feed network (A) connected to the 2-element array, as shown in Figure 3. We denote the ports 1, 2 as the external ports which are connected to the network B and the ports 3, 4 as the internal ports which are connected to the array. We assume that the array can be modeled as a 2-port network with scattering parameter

matrix  $S^a$ :

$$S^a = \begin{bmatrix} S_{11}^a & S_{12}^a \\ S_{21}^a & S_{22}^a \end{bmatrix} \quad (1)$$

The  $S$ -parameters of the feed network A can be denoted by

$$[S] = \begin{bmatrix} S_{11} & S_{12} & S_{13} & S_{14} \\ S_{21} & S_{22} & S_{23} & S_{24} \\ S_{31} & S_{32} & S_{33} & S_{34} \\ S_{41} & S_{42} & S_{43} & S_{44} \end{bmatrix} \quad (2)$$

and the scattering parameter relation for the network A may be expressed as:

$$\begin{bmatrix} b_1 \\ b_2 \\ b_3 \\ b_4 \end{bmatrix} = [S] \begin{bmatrix} a_1 \\ a_2 \\ a_3 \\ a_4 \end{bmatrix} \quad (3)$$

which can be written as:

$$\begin{bmatrix} b_m \\ b_n \end{bmatrix} = \begin{bmatrix} S_{mm} & S_{mn} \\ S_{nm} & S_{nn} \end{bmatrix} \begin{bmatrix} a_m \\ a_n \end{bmatrix} \quad (m = 1, 2, n = 3, 4) \quad (4)$$

$$a_n = S^a b_n \quad b_n = (S^a)^{-1} a_n \quad (5)$$

Combining (5) and the second relation of (4) yields

$$b_n = S_{nm} a_m + S_{nn} a_n = (S^a)^{-1} a_n \quad (6)$$

so that

$$a_n = \left[ (S^a)^{-1} - S_{nn} \right]^{-1} S_{nm} a_m \quad (7)$$

Substituting (7) into the first relation of (4) gives

$$\begin{aligned} b_m &= S_{mm} a_m + S_{mn} a_n = S_{mm} a_m + S_{mn} \left\{ \left[ (S^a)^{-1} - S_{nn} \right]^{-1} S_{nm} a_m \right\} \\ &= \left\{ S_{mm} + S_{mn} \left[ (S^a)^{-1} - S_{nn} \right]^{-1} S_{nm} \right\} a_m = S^c a_m \end{aligned} \quad (8)$$

so that

$$S^c = S_{mm} + S_{mn} \left[ (S^a)^{-1} - S_{nn} \right]^{-1} S_{nm} \quad (9)$$

where  $S^c$  is the scattering parameter matrix of the feed network A and array combination as shown in Figure 3.

Given that  $S_{mm} = S_{nn} = 0$ , calculate  $S^c = S_{mn} S^a S_{nm}$ .

Given that  $S_{mn} = S_{nm}^{-1} = S_{nm}^T$ , calculate  $S^c = S_{nm}^{-1} S^a S_{nm} = \begin{bmatrix} \lambda_1 & 0 \\ 0 & \lambda_2 \end{bmatrix}$ , where  $\lambda$  is the eigenvalue of  $S^a$ . It's noted that due to the

symmetry of the two antennas, thus  $S^a = \begin{bmatrix} S_{11}^a & S_{12}^a \\ S_{21}^a & S_{22}^a \end{bmatrix} = \begin{bmatrix} S_{11}^a & S_{12}^a \\ S_{12}^a & S_{11}^a \end{bmatrix}$  and  $\lambda_1 = S_{11}^a + S_{12}^a$ ,  $\lambda_2 = S_{11}^a - S_{12}^a$ . The input ports of the combined network are therefore decoupled ( $S_{12}^c, S_{21}^c = 0$ ), but mismatched. In addition,  $S_{nm} = [e_1 \ e_2]$ , where  $\mathbf{e}$  is the orthonormal eigenvector of the matrix  $S^a$  while the eigenvectors are given by

$$e_1 = \frac{1}{\sqrt{2}} \begin{bmatrix} 1 \\ 1 \end{bmatrix}, \quad e_2 = \frac{1}{\sqrt{2}} \begin{bmatrix} 1 \\ -1 \end{bmatrix} \tag{10}$$

thus, if the scattering parameter matrix of the feed network A could be satisfied

$$[S] = \frac{1}{\sqrt{2}} \begin{bmatrix} 0 & 0 & 1 & 1 \\ 0 & 0 & 1 & -1 \\ 1 & 1 & 0 & 0 \\ 1 & -1 & 0 & 0 \end{bmatrix} \tag{11}$$

then the input ports of the combined network and array are decoupled.

The feed network (A) for such an array may be implemented with a rat-race 180° hybrid. With port numbering and detailed structure as defined in Figure 4, which is also printed on 1 mm-FR4 substrate. Ports 1, 2 are connected to the network B and the ports 3, 4 are connected to the array, respectively.

To illustrate the scattering parameter matrix of the hybrid, it presents the  $S$  parameters as shown in Figures 5(a), (b), which presents the magnitude and phase characteristics of the  $S$  parameters for the 180° hybrid, respectively. From the figures, it can be observed that it is almost satisfied characteristics of  $[S]$  according to (11).

To validate the principle, we combine the 180° hybrid to our loop-antenna system as shown in Figure 6. It can be observed that

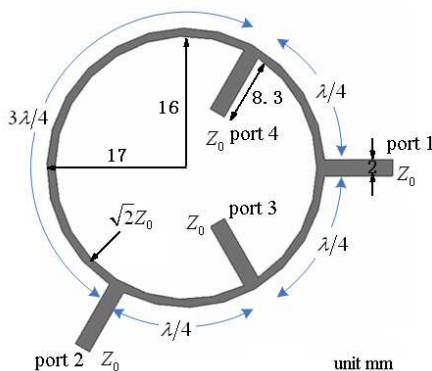
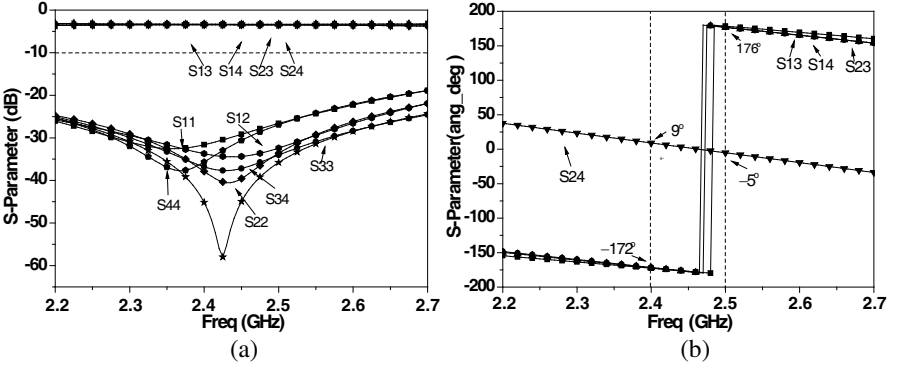
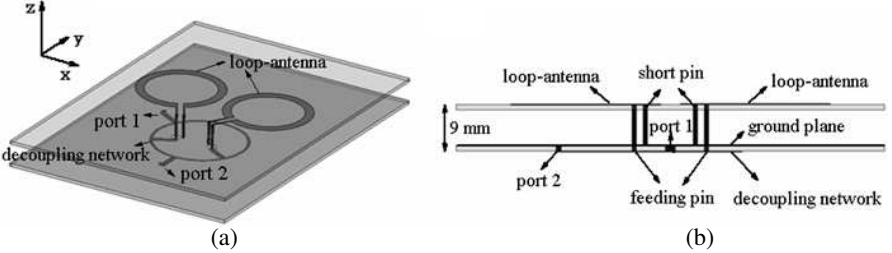


Figure 4. Detailed dimensions of the rat-race 180° hybrid.



**Figure 5.** Simulated  $S$ -parameter for the  $180^\circ$  hybrid (a) magnitude characteristics (b) and phase characteristics.



**Figure 6.** Configuration of the loop-antenna system with decoupling network (a) 3D view (b) Side view.

ports 3, 4 are connected to the proposed antenna through two feeding pins. Figure 7 presents the simulated  $S$  parameter for the combined structure. This is of no surprise, as decoupling should be expected for  $180^\circ$  hybrid, and thus, significant decoupling does occur, which is below  $-20$  dB over 2.4 GHz band. However, mismatch for the port does also occur. They can be matched individually by introducing appropriate matching networks (B).

#### 4. STUDY WITH MATCHING NETWORK

The configuration of the matching networks (B) for such an array is proposed in Figure 8. Firstly, it is find that  $\bar{Y}_1 = 1.06 - 2.62j$ ,  $\bar{Y}_2 = 0.16 - 0.35j$  at 2.45 GHz by HFSS simulation. Then it is obtained values of  $d1 = 29.5$  mm,  $L1 = 5.5$  mm and  $d2 = 20$  mm,  $L2 = 5.2$  mm by means of single stub matching and HFSS optimization, respectively.

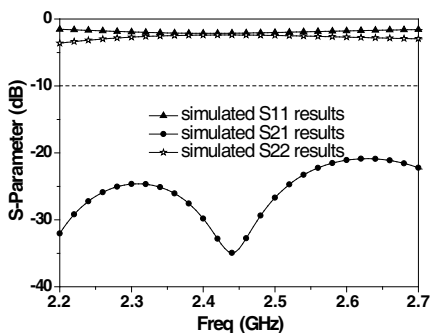


**Figure 7.** Simulated  $S$  parameters for the loop-antenna system with decoupling network.

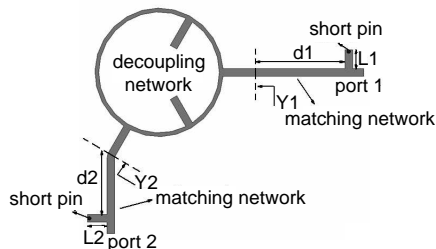


**Figure 8.** Detailed dimensions of the matching networks.

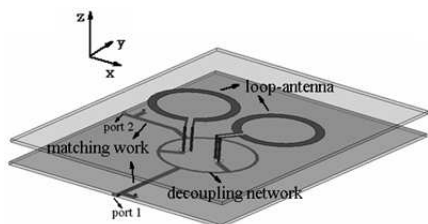


**Figure 9.** Configuration of the loop-antenna system with decoupling and matching networks.



**Figure 10.** Prototype of the proposed antenna.

Figure 9 presents the loop-antenna system with decoupling and matching networks and the antenna prototype fabricated is shown in Figure 10. The  $S$  parameters were measured with Agilent 8722D vector network analyzer. Then Figure 11 shows the measured and simulated  $S$ -parameters against frequency for the two antenna systems. From the figure, it can be observed that measured results reasonably agree with the simulated results well. Mutual coupling across the impedance bandwidth is below  $-20$  dB for the antenna system. Compared with the  $S_{21}$  shown in Figure 2, it is about 17 dB improvements over the antenna system without the networks. Figures 12(a), (b) shows the measured radiation patterns at port 1 and port 2 for the two antenna-system at 2.45 GHz, respectively. The antenna was fed at one of the two input ports of the modal feed network, while the remaining input port was terminated in a matched load. It is seen that the radiation pattern tend to achieve directional radiation, especially in  $x$ - $z$  plane. However, due to the asymmetry of the  $180^\circ$  coupler which results even

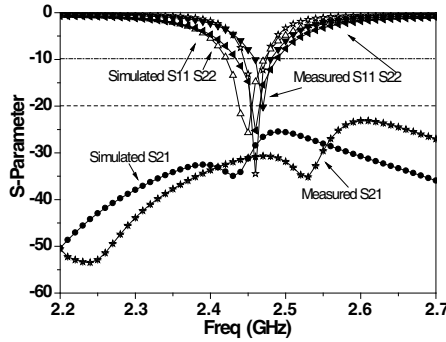


**Figure 11.** Simulated and measured  $S$  parameters for the loop-antenna system with decoupling and matching networks.

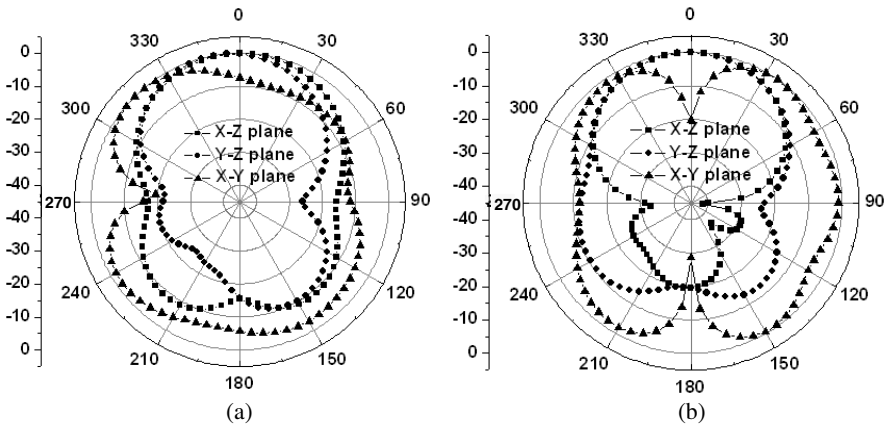


**Figure 12.** Measured radiation pattern at 2.45 GHz (a) fed at port 1 (b) fed at port 2.

and odd modes, the radiation patterns are different from ports 1 and 2 as shown in Figure 12.

The simulated total efficiencies are presented in Figure 13(a). As expected, increasing the isolation between the two antennas results in enhancing their total efficiencies. It can be seen, for the entire bandwidth under consideration, that the total efficiency of the antenna system with decoupling and matching networks is higher than that without decoupling and matching networks. For the two antennas analyzed in this study, the computed envelope correlation coefficients are approximately obtained from the  $S_{ij}$  parameters according to (12) [10]. The envelope correlation coefficient of antenna

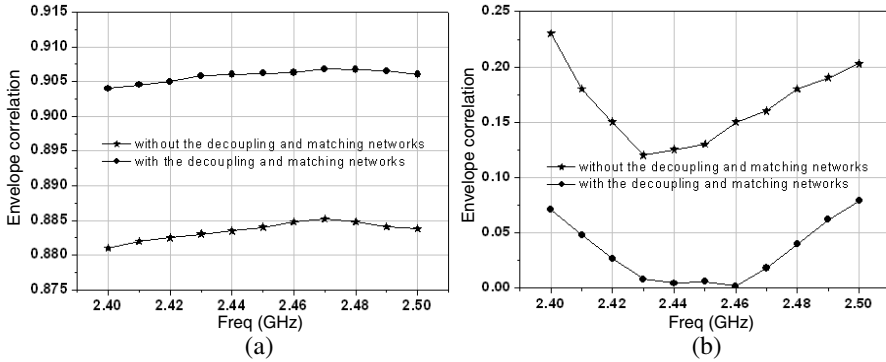


**Figure 13.** (a) Total efficiencies. (b) Envelope correlation.

system with decoupling and matching networks is always lower than the corresponding coefficient of that without decoupling and matching networks in the WLAN 2.4 GHz band as shown in Figure 13(b).

$$\rho_{12} = \frac{|S_{11}^* S_{12} + S_{21}^* S_{22}|^2}{(1 - |S_{11}|^2 - |S_{21}|^2)(1 - |S_{22}|^2 - |S_{12}|^2)} \quad (12)$$

## 5. CONCLUSION

Isolation performances of the printed loop-antenna system for multiple-input multiple-output (MIMO) applications in the 2.4 GHz WLAN band is presented. Results indicate that the isolation  $S_{21}$  between the two antennas (only  $0.07\lambda$  separation) is obviously improved ( $S_{21} < -20$  dB) by using the orthogonality of the eigenmodes of the array based on  $180^\circ$  coupler. Then decoupled external ports of the feed network may be matched independently by using conventional matching circuits well. The antenna is an excellent candidate being embedded inside a wireless access point (AP).

## REFERENCES

1. Su, S.-W. and C.-T. Lee, "Low-cost dual-loop-antenna system for dual-WLAN-band access points," *IEEE Trans. on Antennas and Propag.*, Vol. 59, 1652–1659, 2011.
2. Diallo, A., C. Luxey, P.-L. Staraj, R. Staraj, and G. Kossiavas, "Efficient two-port antenna system for GSM/DCS/UMTS multi-mode mobile phones," *Electronic Letters*, Vol. 43, 369–370, 2007.

3. Diallo, A., C. Luxey, P. L. Thuc, R. Staraj, and G. Kossiavas, "Study and reduction of the mutual coupling between two mobile phone PIFAs operating in the DCS1800 and UMTS bands," *IEEE Trans. Antennas Propag.*, Vol. 54, 2006.
4. Kim, I., C. Won Jung, Y. Kim, and Y. Eil Kim, "Low-profile wideband MIMO antenna with suppressed mutual coupling between two antennas," *Microw. Opt. Technol. Lett.*, Vol. 50, 1336–1339, 2008.
5. Tounou, C., C. Decroze, D. Carsenat, T. Monédière, and B. Jécko, "Diversity antennas efficiencies enhancement," *Proc. IEEE Antennas Propag. Int. Symp.*, 1064–1067, Honolulu, HI, Jun. 2007.
6. Chiu, C.-Y., C.-H. Cheng, R. D. Murch, and C. R. Rowell, "Reduction of mutual coupling between closely-packed antenna elements," *IEEE Trans. on Antennas and Propag.*, Vol. 55, 1732–1738, 2007.
7. Chaloupka, H. J., X. Wang, and J. C. Coetzee, "Superdirective 3-element array for adaptive beamforming," *Microw. Opt. Technol. Lett.*, 425–430, 2003.
8. Chaloupka, H. J., X. Wang, and J. C. Coetzee, "Performance enhancement of smart antennas with reduced element spacing," *Proc. IEEE Conf. Wireless Communications and Networking*, Vol. 1, 425–430, 2003.
9. Anderson, J. B. and H. H. Rasmussen, "Decoupling and descattering networks for antennas," *IEEE Trans. Antennas Propag.*, Vol. 24, 841–846, 1976.
10. Blanch, S., J. Romeu, and I. Corbella, "Exact representation of antenna system diversity performance from input parameter description," *IET Electron. Lett.*, Vol. 39, 705–707, 2003.